

**Identification of functional relevant lysine residues that modulate human farnesoid x receptor
(hFXR) activation**

An-Qiang Sun, Yuhuan Luo, Donald S. Backos, Shuhua Xu, Natarajan Balasubramaniyan, Philip

Reigan and Frederick J. Suchy,

Department of Pediatrics, University of Colorado Anschutz Medical Campus, School of Medicine,
Aurora, CO 80045, (A.S., Y.L., S.X., N.B., F.J.S.)

Skaggs School of Pharmacy and Pharmaceutical Sciences, Department of Pharmaceutical Sciences,
University of Colorado Anschutz Medical Campus, Aurora, CO 80045, (D.S.B., P.R.)

Running Title: role of lysine residues on FXR activation

Corresponding author: An-Qiang Sun, Department of Pediatrics, University of Colorado Denver School of Medicine, Aurora, CO 80045, Phone: (303) 724-5925, Fax: (303)-724-3217, E mail: An-Qiang.Sun@ucdenver.edu

Number of text pager: 26

Number of table: 0

Number of figures: 8

Number of references: 33

Number of words in the abstract: 231

Number of words in the introduction: 443

Number of words in the discussion: 1297

List of Abbreviations:

FXR = farnesoid x receptor

NR = nuclear receptor

OST = organic solute transporter

BSEP = bile salt export pump

SHP = short heterodimer partner

RXR = retinoid X receptor

NaB = sodium butyrate

TSA = trichostatin A

NAM = nicotinamide

HDACi = histone deacetylase inhibitor

CDCA = chenodeoxycholic acid

EMSA = electrophoretic mobility shift assay

DBD = DNA binding domain

LBD = ligand-binding domain

ABSTRACT:

Basic amino acid lysine residues play an important role in regulation of nuclear receptors (e.g. FXR) leading to enhanced or suppressed biological activity. To understand the molecular mechanisms and the subsequent effects in modulating FXR functions in diverse biological processes, we individually replaced eight highly conserved lysine residues of hFXR with arginine. The effects of each mutated FXR on target gene activation, subcellular localization, protein-protein association, and protein-DNA interaction were investigated. Results demonstrated that K122R, K210R, K339R, and K460R mutants of hFXR, significantly impaired target gene (OSTalpha/beta and BSEP) promoter reporter activity in a ligand-dependent fashion. All of the four mutants did not affect the nuclear localization of FXR. Protein interaction studies show that K210R slightly but significantly decreased FXR/RXR binding affinity, but enhanced the interaction of FXR with lysine methyltransferase Set7/9 by ~21%. K460R decreased the FXR interaction with Set7/9 by ~45%, but has no significant effects on interaction with RXR. Electrophoretic mobility shift assays demonstrated that hFXR-K210R and -K339R reduced the protein-DNA (IR1 element at hBSEP promoter) binding affinity by ~80% and ~90%, respectively. Computational-based protein modeling studies were consistent with these results and provided further insights into the potential underlying mechanisms responsible for these results. In conclusion, four highly conserved lysine residues, K122, K210, K339, and K460 of hFXR have been identified that play a critical role in FXR target gene regulation and molecular interaction (protein-protein and protein-DNA).

INTRODUCTION.

The nuclear receptor (NR) farnesoid X receptor (FXR, NR1H4) plays a crucial role in cholesterol and bile acid homeostasis in liver. Recently, the functions of FXR have been extended to glucose and fatty acid metabolism, prevention of gallstone formation, liver regeneration, inhibition of intestinal bacterial growth, and inhibition of inflammation (Hollman et al., 2012; Modica et al., 2010; Zhang and Edwards, 2008). Although such important biological roles of FXR have now been established, the molecular mechanisms of regulating FXR activation are poorly understood.

Previous studies demonstrated that the basic lysine residues of proteins play a crucial role in protein-protein and protein-DNA association (Lu and Hansen, 2003; Sumimoto et al., 2007). The ϵ -amino group of lysine residues often participates in hydrogen bonding and in catalysis of ligand interactions that may be critical for transporter protein function and substrate specificity (Sun et al., 2006). Moreover, many studies show that lysine residues are particularly critical for the posttranslational modifications, such as methylation, acetylation, ubiquitination, and sumoylation (Hollman et al., 2012; Suchy and Ananthanarayanan, 2006). Previous studies have demonstrated that the posttranslational modification at lysine residues are responsible for affecting NR function at multiple levels, e.g. target gene activation, protein association and stability, and protein-DNA interaction (Kemper, 2011; Suchy and Ananthanarayanan, 2006).

Recently, Fang et al. (Fang et al., 2008) showed that the acetylation is critical for ligand-activated FXR induction of small heterodimer partner (SHP/NR0B2). Moreover, Li et al (Li et al., 2007) and Kemper et al (Kemper et al., 2009) reported that SIRT1 [a highly conserved NAD⁺-dependent protein deacetylases] is a positive regulator of liver X receptor (LXR) and FXR. The data from our laboratory also demonstrated that direct methylation of FXR by lysine methyltransferase Set7/9 regulates the expression of FXR target genes (Balasubramaniyan et al., 2012). Posttranslational modifications at

specific lysine residues of NRs provide additional mechanisms for gene specific regulation. Protein sequence prediction analysis suggests that FXR possesses multiple lysine residues within motifs that follow rules for potential posttranslational modification by CBP/p300, SIRT1, Set7/9 and sumoylation etc., and these residues are highly conserved in mammalian and non-mammalian species. However, it is unclear whether these lysine residues are functionally relevant for FXR.

To further understand the molecular mechanisms of lysine modification and the subsequent effects in modulating FXR functions in diverse biological processes, in this study eight highly conserved lysine residues of hFXR have been selected and replaced individually with arginine. The effects of the mutated FXR on target gene activation, protein-protein association, and protein-DNA interaction were assessed. Computational-based protein modeling offered additional mechanistic insights into the functional importance of these residues that may provide possible strategies to selectively control FXR function for therapeutic applications.

MATERIALS AND METHODS:

Plasmid constructs and Site-directed mutagenesis

The full-length coding regions of hFXR α (NR1H4) were amplified by PCR and cloned into KpnI-BamHI sites of pcDNA3.1 (+) Vector (Invitrogen, San Diego, CA), or into PstI-KpnI sites of pEGFP N2 vector (Clontech, Mountain View, CA), respectively, to produce expression construct (pcDNA-hFXR) and green fluorescent protein (GFP) fusion FXR α (hFXR-GFP). The full-length cDNAs of retinoid X receptor (RXR) α and Set7/9, and SHP promoter were generated as described previously (Balasubramaniyan et al., 2012). The luciferase reporter plasmid of human bile salt export pump (hBSEP) was created by inserting its 5'-UTRupstream (from bases -1250 to +65) at NheI-XhoI sites of pGL4.17 [Luc2/neo] vector (Promega, Madison, Wi). hOST α and OST β promoters were kindly provided by Dr Edwards (UCLA, Los Angeles, CA), and inserted at NheI-XhoI sites of pGL4.17 [Luc2/neo] vector (Promega). Selected conserved lysine (Lys, K) residues of hFXR α were mutated to arginine (Arg, R) by site-specific mutagenesis.

Cell culture and Histone deacetylase inhibitors (HDACi) treatment

HepG2 cells (human hepatoblastoma cell line, ATCC, Manassas, VA), CaCo2 cells (human epithelial colorectal adenocarcinoma cells, ATCC, Manassas, VA), and CV-1 (African Green Monkey kidney cell, ATCC, Manassas, VA) were grown in Dulbecco's modified Eagle's medium (DMEM), supplemented with 100 units/ml penicillin/G-streptomycin sulfate and 10% heat-inactivated fetal bovine serum. HepG2 cells were treated with 1 mM sodium butyrate (NaB), 1 μ M trichostatin A (TSA), or 10 mM nicotinamide (NAM), respectively for 6 hr at 37 °C. The mRNA of hBSEP and hSHP in HepG2 cells was quantified by qRT-PCR as described previously (Balasubramaniyan et al., 2005). Fold change values were calculated as the relative expression level compared with that of the cells in the absence of HDACi.

Transient transfections and reporter gene assays

CV-1 cells were co-transfected with hBSEP promoter reporters, hRXR α and hFXR α constructs. The cotransfected cells were treated with 100 μ M chenodeoxycholic acid (CDCA) for 20 hours at 37 °C. Transfection efficiencies were normalized using β -galactosidase. After treated with HDACi for 6 hr at 37 °C, the cells were collected for the luciferase activity assay. Similarly, in HepG2 and CaCo2 cells, transient transfections were performed on 48-well. 24 hours after transfection, medium was refreshed and supplemented with 50 μ M CDCA. Cells were harvested after 24 hours for determination of luciferase activity. Transfection efficiencies were normalized using β -galactosidase. Each transfection was performed in triplicate, and experiments were repeated at least three times. The EC50 values were determined and calculated as described by Grienke et al (Grienke et al., 2011).

Confocal microscopy

The GFP fused hFXR α plasmid (hFXR-GFP) and mutants were transiently co-transfected with hRXR α to HepG2 cells. Cell culture and DNA transfection of cells were performed as described previously (Sun et al., 2004). Fluorescence was examined with a Leica TCS-SP (UV) four-channel confocal laser scanning microscope.

Mammalian two-hybrid (M2H) analysis

The mammalian two-hybrid assay was performed by the modified Checkmate mammalian two hybrid system (Promega), as used previously (Balasubramanian et al., 2012; Sun et al., 2007). Briefly, transient transfections were performed on 48-well. HepG2 cells were cotransfected with the pBIND/FXR (containing WT or mutants), pACT/Set7/9 or pACT/RXR α , pG5/luc and pCMV- β galactosidase plasmids by using TransIT-LT (Mirus Bio, Madison, WI). 24 hours after transfection,

medium was refreshed and supplemented with 50 μ M CDCA. After additional 24 h incubation, cells were harvested for determination of luciferase activity by luminometer (Promega). The transfection efficiency was normalized using β -galactosidase activity.

Electrophoretic mobility shift assays (EMSA)

EMSA analysis was performed as described previously (Balasubramaniyan et al., 2012). Briefly, cDNAs encoding human RXR α , hFXR α and mutated FXR α were transcribed and translated by the TNT-coupled reticulocyte lysate system (Promega). EMSA assays were conducted by aliquots of the transcribed/translated extracts. Oligonucleotide probes for the EMSAs were end-labeled with [γ - 32 P]ATP (3000 or 6000 mCi/mmol) by T4 polynucleotide kinase. In competition assays, unlabeled wild type or mutant oligonucleotides were added to the reaction mix for 15 min before the addition of the probe. DNA-protein complexes were resolved on 4% native polyacrylamide gel electrophoresis containing 0.5x TBE. The gel was dried and exposed to x-ray film. Quantitation of the retarded complex was done by scanning the X-ray films and using ImageJ software (<http://rsb.info.nih.gov/ij/>). Competitor oligonucleotides used for EMSA including the wild type or mutated hBSEP FXRE (IR1) sequences, wild type GGACTTTAGGCCATTGACCTATAAGCAA, Mutant GGACTTTAaaCCATTGAttTATAAGCAA.

Computational-based molecular modeling of hFXR

All molecular modeling studies were conducted using Accelrys Discovery Studio 3.1 (Accelrys Software, Inc., San Diego, CA; <http://accelrys.com>). Crystal structure coordinates were obtained from the protein data bank (<http://www.pdb.org>). The protein homology model of the hFXR was constructed using the MODELLER protocol (Eswar et al., 2006) using crystal structures of the hFXR ligand binding domain (PDB ID: 1OSH, 3BEJ; 100% sequence identity) (Downes et al., 2003; Soisson et al., 2008) and

the crystal structure of the DNA binding domain (DBD) from the retinoid-x-receptor (PDB ID: 3DZY; 37% identity, 55% similarity vs. the hFXR DBD) (Chandra et al., 2008). Structural coordinates of the bound DNA from the RXR crystal structure were transferred into the homology model during model construction. No suitable templates for residues 1-124 of hFXR were identified and these residues have therefore been omitted from the model. The structure was then subjected to loop refinement with the DOPE energy function (Shen and Sali, 2006) prior to a final energy minimization using the conjugate gradient minimization protocol (10,000 iterations to a gradient tolerance of 0.001 kcal/mol) with a CHARMM forcefield and the Generalized Born implicit solvent model with simple switching (Feig et al., 2004). Hypothetical models of possible protein-protein interactions between FXR and the Set7/9 methyltransferase were constructed by aligning the relevant 4 amino acid residues of FXR (Lys204-Arg207, Asp458-Phe461, or Thr462-His459) over the residues in the -2 through +1 positions (with the methylated Lys residue occupying the 0 position) of the histone H3 peptide fragment (Arg2-Gln5) from the crystal structure of the Set7/9-histone H3 ternary complex (PDB ID: 1O9S) (Xiao et al., 2003)(PDB ID: 1O9S). The resulting complexes were then subjected to energy minimization as described above. The predicted alterations in response to the K210R mutation were examined by changing this residue in the hypothetical FXR(206)-Set7/9 complex to the mutant form and subjecting both the WT and mutant complexes to a further round of minimization as described above.

Statistical analysis

Data are presented as the mean +/- the standard deviation (SD) determined by the analysis of multiple independent samples, each assayed in duplicate or triplicate, as indicated in the figure legends. A two-tailed Student's t-test was used to calculate *p* values.

RESULTS:

Histone deacetylase inhibitors (HDACi) enhance endogenous expression of hFXR targeted genes.

Previous studies demonstrated that FXR acetylation is regulated by the class III deacetylase SIRT1 at K213 (Kemper et al., 2009). To determine whether modification of hFXR by class I and II deacetylases are functionally relevant to its target gene (hBSEP and SHP) expression, we first tested the effects of sodium butyrate (NaB), trichostatin A (TSA), and nicotinamide (NAM) on expression of FXR target genes. NaB and TSA (both are class I and II HDACi) and NAM (a class III HDACi) disrupt normal chromatin structure and protein deacetylation by different mechanisms, and cause alterations in gene expression and regulation. HepG2 cells were treated with HDACi for 6 hr at 37 °C. qRT-PCR was used to determine the mRNA expression of the target genes. The results (Figure 1) demonstrated that after 6 hr treatment of HepG2 cells with NaB or NAM, endogenous BSEP mRNA level increased ~2.5-fold and ~1.5-fold respectively, compared with untreated cells. Similarly, after 6 hr treatment with NaB or NAM, endogenous SHP mRNA level increased ~1.5-fold and ~1.8-fold respectively. The TSA treatment has no significant effect. These results suggest that not only class III (SIRT1), but also class I and II deacetylases may be involved in bile acid-activated FXR signaling *in vivo*.

The importance of several conserved lysine mutations of hFXR α on ligand-dependent transactivation of hBSEP, hOST α , and hOST β promoters.

Previous studies have demonstrated that K206 and K213 of hFXR α may be methylated and acetylated, respectively (Balasubramanian et al., 2012; Kemper et al., 2009). In hFXR α several lysine residues, including K122, K210, and K237, have been identified as potential substrates for acetylation that may lead to activation of the target genes (Fu et al., 2004; Kimura et al., 2005). Recent evidence also indicates that a single lysine is conserved among nuclear receptors (K460 in humans, K432 in mice), and is subject to deacetylation by the NAD⁺-dependent deacetylase SIRT1 leading to activation of the

nuclear receptor LXR (Li et al., 2007). The structure prediction and modeling studies indicate that eight lysine residues of hFXR (K122, K157, K206, K210, K213, K237, K339, and K460) are highly conserved, located on the ligand or DNA binding domain, and may be involved in protein-protein and/or protein-DNA interactions. Some of the eight lysine-residues may also potential sumoylation sites and exhibit some overlap with the acetylation sites. Therefore, the eight lysine residues of hFXR were selected, and individually replaced with arginine (Figure 2). The subsequent effects on the transactivation of target gene expression were examined in transfected HepG2 and CaCo2 cells for hOST α and β , and in HepG2 cells for BSEP.

Transfection of wild type hFXR α markedly increased the transactivation of the target gene promoters (Figure 3). After treatment with 50 μ M of CDCA (a primary bile acid), the transactivations of hBSEP, hOST α and β promoters were further enhanced about 3-fold compared with untreated cells. Replacement of the conserved residues K122, K210 and K339 of hFXR with arginine significantly reduced the CDCA ligand-induced activation of the hOST α promoter activity by ~19%, ~26% and ~48%, respectively, in transfected HepG2 cells, and by ~30%, ~34% and ~60%, respectively, in transfected CaCo2 cells compared with the cells transfected with wild type FXR (Figure 3A). The K460R mutant slightly decreased the hOST α promoter activity by ~10% in HepG2 cells, but had no effect in CaCo2 cells (Figure 3A). The K122R, K210R, K339R, and K460R mutants exhibited decreased ligand-induced activation of the hOST β promoter activity by ~31%, ~11%, ~65%, and ~26%, respectively, in transfected HepG2 cells, and by ~31%, ~21%, 54% and ~20%, respectively, in transfected CaCo2 cells compared with the cells transfected with wild type FXR (Figure 3B). In contrast, K157R and K206R mutants enhanced the CDCA ligand-induced activation of the hOST β promoter activity by ~38% and ~41%, respectively, in transfected HepG2 and CaCo2 cells (Figure 3B). It is notable that the ligand untreated basal reporter activity of some of the mutants were changed, in

particular the K157R and K213R in OST β -HepG2, compared with the wild type FXR. This suggests that these mutations of FXR may induce a functional change that is ligand independent for interacting with hOST β promoter. For hBSEP promoter, K122R, K210R, K339R, and K460R mutants decreased the CDCA ligand-induced activation by ~59%, ~54%, 66% and ~40%, respectively, in transfected HepG2 cells (Figure 3C). These data suggest that the conserved lysines, K122, K210, K339, and K460 are critically important for optimal ligand-activated FXR signaling and we chose to focus on these four lysine residues in the following studies.

The nuclear trafficking of GFP-tagged hFXR is not affected by mutation of selected conserved lysine residues.

The posttranslational modification of a protein could determine its transcriptional activity through effects on subcellular localization, binding to DNA, and/or interaction with transcriptional coactivators. To understand the mechanism of the CDCA-mediated FXR signaling in HepG2 cells, we first examined whether the site directed mutagenesis alters the subcellular distribution of GFP-FXR. In transfected HepG2 cells, all of the wild type and mutant GFP-FXR proteins translocated into the nucleus, indicating that the mutation of hFXR at either K122, K210, K339, or K460 did not interrupt hFXR nuclear trafficking (Supplemental Figure 1).

The effects of selected conserved lysine mutants of hFXR on protein-protein interaction with RXR and the methyltransferase Set7/9.

Several proteins interact with hFXR, including RXR and Set7/9, to form a transcriptional complex that regulates the target gene expression (Balasubramanian et al., 2012; Vaz and de Lera, 2012). Recently, evidence indicated that K206 and K213 residues of hFXR are a target of the lysine methyltransferase Set7/9 and the NAD⁺-dependent deacetylase SIRT1, respectively (Balasubramanian et al., 2012;

Kemper et al., 2009). However, whether these lysine residues are involved in the interaction with other cofactors are unknown. To further understand the mechanisms of the ligand-activated FXR signaling, the effects of the lysine mutants on FXR/RXR and FXR/Set7/9 protein interaction were analyzed by mammalian two-hybrid analysis. The K206R and K210R mutants modestly but significantly decreased the ligand induced interaction between FXR and RXR by ~28% and ~10%, respectively (Figure 4A). The K206R and K460R mutants each decreased the ligand induced FXR/Set7/9 interaction by ~45% (Figure 4B). In contrast, the K210R mutant enhanced the ligand induced FXR/Set7/9 binding affinity by ~21%. This is consistent with our previous results for K206 (Balasubramaniyan et al., 2012), and further suggests that K210 and K460 may also be targets for Set7/9-mediated FXR methylation.

Conserved lysine mutants of hFXR decrease the binding affinity with target gene promoter binding element, BSEP-FXRE (IR-1).

Since the lysine modification of FXR may determine its transcriptional activity through effects on the binding affinity for the IR1 element in hBSEP promoter, an electrophoretic mobility shift assay (EMSA) was performed. EMSA analysis carried out using *in vitro* translated wild type and mutated FXR. Figure 5 demonstrated that the hFXR-K210R and -K339R mutants reduced the protein-DNA (IR1 element at hBSEP promoter) interaction by ~80%, and ~90%, respectively, while the hFXR-K122R, K237R, and K460R mutants had equivalent binding to IR1 element compared with wild type FXR. These data suggested that K210 and K339 may be directly or indirectly involved in the protein-DNA binding processes.

Computational-based modeling of FXR.

In order to examine possible mechanisms by which these mutations alter FXR function, we performed a series of computational-based molecular modeling studies. As the crystal structure of the hFXR

containing an intact DNA-binding domain has not yet been determined, we began by constructing a homology model of the overall structure (residues 125-472) using crystal structures of the hFXR ligand binding domain and the DNA binding domain from human RXR, as described in the methods. The model revealed that K206 and K210 are located in positions with the potential to directly interact with the DNA strand (Figure 6A). Interestingly, K210 is predicted to be involved in hydrogen bond interactions with two phosphate groups on the DNA backbone (Figure 6B). The K339 residue is situated in the ligand binding domain at the entrance to the ligand binding pocket, while the K460 resides at the interaction interface where the FXR may associate with other co-factors (Figure 6A). Although our model does not include K122, the model N-terminus (Glu125) is identified and its location suggests K122 also has the potential to directly interact with the DNA strand (Figure 6B).

DISCUSSION:

FXR acts as a bile acid sensor inducing the transcription of multiple genes involved in the bile acid homeostasis within the hepatocyte. FXR contains a number of domains, including a DNA binding domain (DBD), a hinge region, a dimerization interface, and a ligand-binding domain (LBD)(Lee et al., 2006). Amino acid sequence prediction analysis suggests that FXR possesses multiple potential lysine modification sites for acetylation, methylation and/or sumoylation. This study suggested that similar to the type III deacetylase SIRT1, the type I and II deacetylases may also be involved in FXR acetylation/deacetylation processes. However, whether these potential lysine modification sites of FXR are functionally relevant, and the mechanisms underlying the lysine modification-induced alterations in activity are still not fully understood.

The results of current study demonstrated that individual replacement of K122, K210, K339, and K460 of hFXR with arginine significantly reduced target gene promoter reporter activity in a ligand-dependent fashion, but did not affect the nuclear localization of FXR. This suggests that reduction of the target gene activation by these mutants is not due to the interruption of subcellular trafficking. Functional changes of NRs by lysine mutation may be induced by an apparent conformational change that modulates the protein association with cellular co-factors to alter the nuclear localization, the binding and recruitment of coactivators and corepressors to target gene promoters, and the DNA binding activity of various transcription factors. (Soutoglou et al., 2000).

FXR-K210 is located in the hinge region between a methylation site at K206 and an acetylation site at K213. Our results demonstrated that mutation of K210 to arginine results in a significant reduction of the activity in the target gene expression, particularly to BSEP promoter. The K210R mutation results in a slight but significant decrease in FXR/RXR binding affinity, but enhanced FXR/Set7/9 interaction.

This mutation also dramatically decreases the interaction between FXR and the BSEP-promoter (FXRE). Our computational-based modeling suggests that K210 may participate in direct hydrogen-bond interactions with the DNA backbone by the ϵ -amino group. This flexible hinge region of FXR may also be involved in heterodimer formation with RXR, and/or interaction with the methyltransferase Set7/9. A coiled-coil type structure is important for protein association, and many coiled-coil type proteins are involved in important biological functions such as the regulation of gene expression, e.g. transcription factors. Prediction of coiled-coil regions in hFXR shows that the hinge region (amino acid 175 to 225) of hFXR has high potential to form a coiled-coil structure (Supplemental Figure 2) [http://www.ch.embnet.org/software/COILS_form.html]. Replacement of the K206 with Arg could decrease the coiled-coil structure by ~16%. In contrast, replacement of the K210 with Arg could enhance the coiled-coil structure by ~6.3%. These data are consistent with our results, and suggest that K210 is important for both the protein-protein and protein-DNA interaction.

FXR-K339 is located in the LBD, and is a potential modification site for both acetylation and sumoylation. Our results demonstrate that arginine replacement of K339 resulted in a decrease in the activation of the promoters of three target genes (OST α , OST β and BSEP) in HepG2 (liver) and CaCo2 (intestine) cell lines. This mutation almost completely abolished the FXR interaction with the BSEP-promoter, but did not cause significant effects on the protein-protein interaction with either RXR or Set7/9. Our modeling indicates that K339 is located at the entrance of the ligand-binding site of FXR, suggesting that substitution of the Lys with the bulkier side chain of an Arg residue may impede access to the ligand-binding site. Therefore, the observed inhibition of activity may be due, at least in part, to impaired ligand binding to FXR. This is consistent with the results of EC50 (data not show) that suggest the K339R mutant significantly reduced the ligand binding affinity.

The K460R mutation significantly decreased the transactivation of OST α , OST β and BSEP promoters, in HepG2 cells. The mutation decreased the transactivation of OST β but not OST α promoter in CaCo2 cells. K460R also dramatically decreased the FXR interaction with Set7/9, but had no significant effect on the interaction with RXR. In contrast with the K210R and K339R mutants, EMSA study shows that the K460R mutant did not effect FXR-DNA interaction. Previous studies reported the similar observation that acetylation of mouse GATA-1 or EKLF is important for transcriptional activation without affecting their DNA binding activities (Hung et al., 1999; Zhang and Bieker, 1998). Taken together, these data suggest that K460 may be critical for the FXR specificity in modulating different target gene activities and biological processes.

K122 is a potential acetylation site and a strong sumoylation candidate. Although our model does not include K122, it is in close proximity to the N-terminus of our model (Glu125) and therefore may also be involved in DNA binding.

Set7/9 is known to methylate a number of cellular protein targets, including histone H3, p53, and NF- κ B (Del Rizzo and Trievel, 2011) and we have previously shown that FXR is a target of Set7/9-mediated methylation at K206 (Balasubramaniyan et al., 2012). Our *in vitro* data demonstrates the K210R and K460R mutations alter the interaction of FXR with Set7/9, which support our finding regard methylation of K210 and suggests that K460 may be involved in FXR methylation. It was therefore of interest to examine whether the interaction between Set7/9 and FXR was feasible, specifically the two regions of FXR containing K206 and K460, and whether this interaction was sufficient to result in the methylation of these residues. Most Set7/9 methylation sites conform to a conserved recognition sequence motif of (K/R)-(S/T/A)-K-X, where the underlined Lys residue is the methylated species and X is a polar residue (Couture et al., 2006; Del Rizzo and Trievel, 2011). The protein sequence in the region containing

K206 (204-KSKR-207) matches this recognition sequence. The flexible nature of the FXR hinge domain which contains K206 also allows this residue to be well positioned in the binding site of Set7/9 for its methylation and results in favorable electrostatic interactions between the two proteins (Figure 7). The sequence around K460 (458-DHKF-461) is not similar to the Set7/9 recognition sequence in the N-terminal to C-terminal orientation but does exhibit similarity at the +1 position in the opposite C-terminal to N-terminal orientation (462-TFKH-459). The role of K460 in this process is unclear.

Interestingly, the K210R mutant induced a small but significant increase in the interaction between FXR and Set7/9 in our two hybrid screen. We examined the effect of this mutation *in silico* by mutating the residue to an Arg in our hypothetical model of the FXR(206)-Set7/9 protein complex and subjecting both the wild-type and K210R mutant to a further round of energy minimization. Although the side chain of the residue at this position does not appear to be involved in direct interactions with Set7/9, the Arg substitution is predicted to result in the introduction of additional hydrogen bond interactions with the side chain carbonyl of Asn211 (Figure 8). In our model, the side chain amine of Asn211 is also predicted to be involved in hydrogen bond interactions with Asp338 of Set7/9. These additional predicted interactions may introduce additional stability to this flexible region of FXR that may help to explain the mildly enhanced interaction between FXR and Set7/9 we observed *in vitro* in response to the K210R mutation. However, the physiological relevance of such a modest increase in activity is unclear and may not play a significant role in Set7/9-mediated methylation of FXR within the cellular milieu.

In summary, we have identified four highly conserved lysine residues, K122, K210, K339, and K460 that play a critical role in FXR target gene regulation and molecular interaction (protein-protein and protein-DNA) in a ligand-dependent manner. Our data further demonstrates that class I, II, III HDAC

inhibitors have variable effects on *in vivo* BSEP mRNA expression. Thus, FXR contains multiple potential acetylation sites that may be differentially important depending on the gene and cellular content.

ACKNOWLEDGMENTS

The authors gratefully acknowledge Dr. PA Edwards (University of California, Los Angeles, Los Angeles, CA) for the kindly provide OST α and β promoter constructs, and Mr. Jaeyong Ahn (Mount Sinai School of Medicine, New York, New York) for the assistance to initiate some of the experiments. The authors would also like to thank the Computational Chemistry and Biology Core Facility at University of Colorado Anschutz Medical Campus for their contributions to this manuscript.

Authorship contributions:

Participated in research design: Sun, Suchy

Conducted experiments: Sun, Luo, Xu, Balasubramaniyan,

Conducted computation structure modeling: Backos, Reigan

Performed data analysis: Sun, Suchy

Wrote or contributed to the writing of the manuscript: Sun, Suchy, Backos, Reigan

REFERENCES:

- Balasubramaniyan N, Ananthanarayanan M and Suchy FJ (2012) Direct methylation of FXR by Set7/9, a lysine methyltransferase, regulates the expression of FXR target genes. *Am J Physiol Gastrointest Liver Physiol* **302**(9): G937-947.
- Balasubramaniyan N, Shahid M, Suchy FJ and Ananthanarayanan M (2005) Multiple mechanisms of ontogenic regulation of nuclear receptors during rat liver development. *Am J Physiol Gastrointest Liver Physiol* **288**(2): G251-260.
- Chandra V, Huang P, Hamuro Y, Raghuram S, Wang Y, Burris TP and Rastinejad F (2008) Structure of the intact PPAR-gamma-RXR- nuclear receptor complex on DNA. *Nature* **456**(7220): 350-356.
- Couture JF, Collazo E, Hauk G and Trievel RC (2006) Structural basis for the methylation site specificity of SET7/9. *Nat Struct Mol Biol* **13**(2): 140-146.
- Del Rizzo PA and Trievel RC (2011) Substrate and product specificities of SET domain methyltransferases. *Epigenetics* **6**(9): 1059-1067.
- Downes M, Verdecia MA, Roecker AJ, Hughes R, Hogenesch JB, Kast-Woelbern HR, Bowman ME, Ferrer JL, Anisfeld AM, Edwards PA, Rosenfeld JM, Alvarez JG, Noel JP, Nicolaou KC and Evans RM (2003) A chemical, genetic, and structural analysis of the nuclear bile acid receptor FXR. *Mol Cell* **11**(4): 1079-1092.
- Eswar N, Webb B, Marti-Renom MA, Madhusudhan MS, Eramian D, Shen MY, Pieper U and Sali A (2006) Comparative protein structure modeling using Modeller. *Curr Protoc Bioinformatics* **Chapter 5**: Unit 5 6.
- Fang S, Tsang S, Jones R, Ponugoti B, Yoon H, Wu SY, Chiang CM, Willson TM and Kemper JK (2008) The p300 acetylase is critical for ligand-activated farnesoid X receptor (FXR) induction of SHP. *The Journal of biological chemistry* **283**(50): 35086-35095.
- Feig M, Onufriev A, Lee MS, Im W, Case DA and Brooks CL, 3rd (2004) Performance comparison of generalized born and Poisson methods in the calculation of electrostatic solvation energies for protein structures. *J Comput Chem* **25**(2): 265-284.
- Fu M, Wang C, Zhang X and Pestell RG (2004) Acetylation of nuclear receptors in cellular growth and apoptosis. *Biochem Pharmacol* **68**(6): 1199-1208.
- Grienke U, Mihaly-Bison J, Schuster D, Afonyushkin T, Binder M, Guan SH, Cheng CR, Wolber G, Stuppner H, Guo DA, Bochkov VN and Rollinger JM (2011) Pharmacophore-based discovery of FXR-agonists. Part II: identification of bioactive triterpenes from *Ganoderma lucidum*. *Bioorg Med Chem* **19**(22): 6779-6791.
- Hollman DA, Milona A, van Erpecum KJ and van Mil SW (2012) Anti-inflammatory and metabolic actions of FXR: insights into molecular mechanisms. *Biochim Biophys Acta* **1821**(11): 1443-1452.
- Hung HL, Lau J, Kim AY, Weiss MJ and Blobel GA (1999) CREB-Binding protein acetylates hematopoietic transcription factor GATA-1 at functionally important sites. *Mol Cell Biol* **19**(5): 3496-3505.
- Kemper JK (2011) Regulation of FXR transcriptional activity in health and disease: Emerging roles of FXR cofactors and post-translational modifications. *Biochim Biophys Acta* **1812**(8): 842-850.
- Kemper JK, Xiao Z, Ponugoti B, Miao J, Fang S, Kanamaluru D, Tsang S, Wu SY, Chiang CM and Veenstra TD (2009) FXR acetylation is normally dynamically regulated by p300 and SIRT1 but constitutively elevated in metabolic disease states. *Cell Metab* **10**(5): 392-404.
- Kimura A, Matsubara K and Horikoshi M (2005) A decade of histone acetylation: marking eukaryotic chromosomes with specific codes. *J Biochem* **138**(6): 647-662.

- Lee H, Zhang Y, Lee FY, Nelson SF, Gonzalez FJ and Edwards PA (2006) FXR regulates organic solute transporters alpha and beta in the adrenal gland, kidney, and intestine. *J Lipid Res* **47**(1): 201-214.
- Li X, Zhang S, Blander G, Tse JG, Krieger M and Guarente L (2007) SIRT1 deacetylates and positively regulates the nuclear receptor LXR. *Mol Cell* **28**(1): 91-106.
- Lu X and Hansen JC (2003) Revisiting the structure and functions of the linker histone C-terminal tail domain. *Biochem Cell Biol* **81**(3): 173-176.
- Modica S, Gadaleta RM and Moschetta A (2010) Deciphering the nuclear bile acid receptor FXR paradigm. *Nucl Recept Signal* **8**: e005.
- Rahman MM, Kukita A, Kukita T, Shobuike T, Nakamura T and Kohashi O (2003) Two histone deacetylase inhibitors, trichostatin A and sodium butyrate, suppress differentiation into osteoclasts but not into macrophages. *Blood* **101**(9): 3451-3459.
- Shen MY and Sali A (2006) Statistical potential for assessment and prediction of protein structures. *Protein Sci* **15**(11): 2507-2524.
- Soisson SM, Parthasarathy G, Adams AD, Sahoo S, Sitlani A, Sparrow C, Cui J and Becker JW (2008) Identification of a potent synthetic FXR agonist with an unexpected mode of binding and activation. *Proc Natl Acad Sci U S A* **105**(14): 5337-5342.
- Soutoglou E, Katrakili N and Talianidis I (2000) Acetylation regulates transcription factor activity at multiple levels. *Mol Cell* **5**(4): 745-751.
- Suchy FJ and Ananthanarayanan M (2006) Bile salt excretory pump: biology and pathobiology. *J Pediatr Gastroenterol Nutr* **43 Suppl 1**: S10-16.
- Sumimoto H, Kamakura S and Ito T (2007) Structure and function of the PB1 domain, a protein interaction module conserved in animals, fungi, amoebas, and plants. *Sci STKE* **2007**(401): re6.
- Sun AQ, Balasubramanian N, Chen H, Shahid M and Suchy FJ (2006) Identification of functionally relevant residues of the rat ileal apical sodium-dependent bile acid cotransporter. *J Biol Chem* **281**(24): 16410-16418.
- Sun AQ, Balasubramanian N, Liu CJ, Shahid M and Suchy FJ (2004) Association of the 16-kDa subunit c of vacuolar proton pump with the ileal Na⁺-dependent bile acid transporter: protein-protein interaction and intracellular trafficking. *J Biol Chem* **279**(16): 16295-16300.
- Sun AQ, Balasubramanian N, Xu K, Liu CJ, Ponamgi VM, Liu H and Suchy FJ (2007) Protein-protein interactions and membrane localization of the human organic solute transporter. *Am J Physiol Gastrointest Liver Physiol* **292**(6): G1586-1593.
- Vaz B and de Lera AR (2012) Advances in drug design with RXR modulators. *Expert Opin Drug Discov*.
- Xiao B, Jing C, Wilson JR, Walker PA, Vasisht N, Kelly G, Howell S, Taylor IA, Blackburn GM and Gamblin SJ (2003) Structure and catalytic mechanism of the human histone methyltransferase SET7/9. *Nature* **421**(6923): 652-656.
- Zhang W and Bieker JJ (1998) Acetylation and modulation of erythroid Kruppel-like factor (EKLF) activity by interaction with histone acetyltransferases. *Proc Natl Acad Sci U S A* **95**(17): 9855-9860.
- Zhang Y and Edwards PA (2008) FXR signaling in metabolic disease. *FEBS Lett* **582**(1): 10-18.

Footnotes.

This work was supported in part by the National Institutes of Health Grant [DK084434-28] to F. J. S.

Figure Legends:

Figure 1: Effects of histone deacetylase inhibitors (HDACi) on the endogenous expression of hBSEP and hSHP mRNA:

HepG2 (human hepatoblastoma) cells were treated with 1 mM Na-butyrate (NaB), 1 μ M trichostatin A (TSA), and 10 mM nicotinamide (NAM), respectively for 6 hr at 37 °C. The mRNA expressions of human BSEP (Top) and SHP (Lower) were determined by Quantitative Real-Time PCR, and optical density of the PCR products was normalized to the expression of glyceraldehydes-3-phosphate dehydrogenase (GAPDH). Fold change values were calculated as the relative expression level compared with that of the cells in the absence of HDAC inhibitors. (* $p \leq 0.05$, compared with HDAC non-treated cells)

Figure 2. Sequence alignment of FXR from different species.

The star (*) indicated selected potential posttranslational modification lysine residues.

Figure 3. The importance of several conserved lysine mutations of hFXR α on ligand-dependent transactivation of hBSEP, hOST α , and hOST β promoters.

Human OST α (-1489 to +112 bp)(A), OST β (-529 to +17 bp)(B), and BSEP (-1250 to +65 bp)(C) promoters fused with luciferase reporter were cotransfected with hRXR α and wild type or mutated hFXR α constructs in HepG2 or CaCo2 cells. 24 hr later, cells were incubated with vehicle (DMSO) or with 50 μ M CDCA for an additional 16 hr and analyzed for luciferase activity. Transfection efficiencies were normalized using β -gal. (* $p \leq 0.05$, compared with WT FXR)

Figure 4. Effects of site directed mutagenesis at conserved lysine residues of human FXR on protein-protein interaction.

Mammalian two-hybrid analysis was performed in co-transfected HepG2 cells (see Method section), and used to evaluate the effects of the mutations on the association of hFXR α with (A) hRXR α and (B) Set7/9. (* $p \leq 0.05$, compared with WT FXR)

Figure 5. Effects of site directed mutagenesis at conserved lysine residues of human FXR on Binding to FXRE of hBSEP promoter.

(A) Electrophoretic mobility shift assay (EMSA) analysis using in vitro translated wild type and mutated FXR and wild type RXR using ^{32}P -labeled FXRE (IR-1) as a probe. Note the absence of specific DNA-protein complex in the lanes (indicated by asterisk) when K210R or K339R mutants were used in the reaction. (-Sp = Specific complexes, and -NSp = non-specific complexes). (B) Quantification of the density of Protein-DNA complexes from (A). (* $p \leq 0.05$, compared with WT FXR)

Figure 6. Identifying the locations of four critical lysine residues in the structure of human FXR.

(A) Protein homology model of ligand, hinge, and DNA binding domains of human FXR (cyan ribbons) bound to DNA (multi-colored sticks) with the locations of the relevant Lys residues (yellow sticks) and the interaction interface with protein co-factors indicated. The asterisk (*) denotes the location of the FXR ligand binding pocket. (B) Close up view of the DNA-binding domain from A depicting the locations of the homology model N-terminus (Glu125) and two Lys residues that may be involved in DNA binding. Green lines represent predicted hydrogen bond interactions with the phosphate backbone of DNA.

Figure 7. Hypothetical structures of the FXR-Set7/9 protein complexes.

Energy minimized structures of Set7/9 bound to FXR at Lys206. Set7/9 protein surfaces are colored by interpolated surface charge in a range from positive (blue) to neutral (white) to negative (red). FXR protein surfaces are colored similarly excepting that neutral areas are colored green to distinguish the surface from that of Set7/9. The potential methylated Lys residues are indicated in the respective insets.

Figure 8. Predicted effects of the K210R mutation on the interaction between FXR and Set7/9.

Predicted interactions between FXR (green) and Set7/9 (white) in the hypothetical model of the FXR-Set7/9 complex containing either (A) wild-type FXR or (B) K210R FXR. Green lines denote predicted hydrogen bond interactions and orange lines denote predicted pi bond interactions. Labels in italics indicate Set7/9 residues.

Figure 1

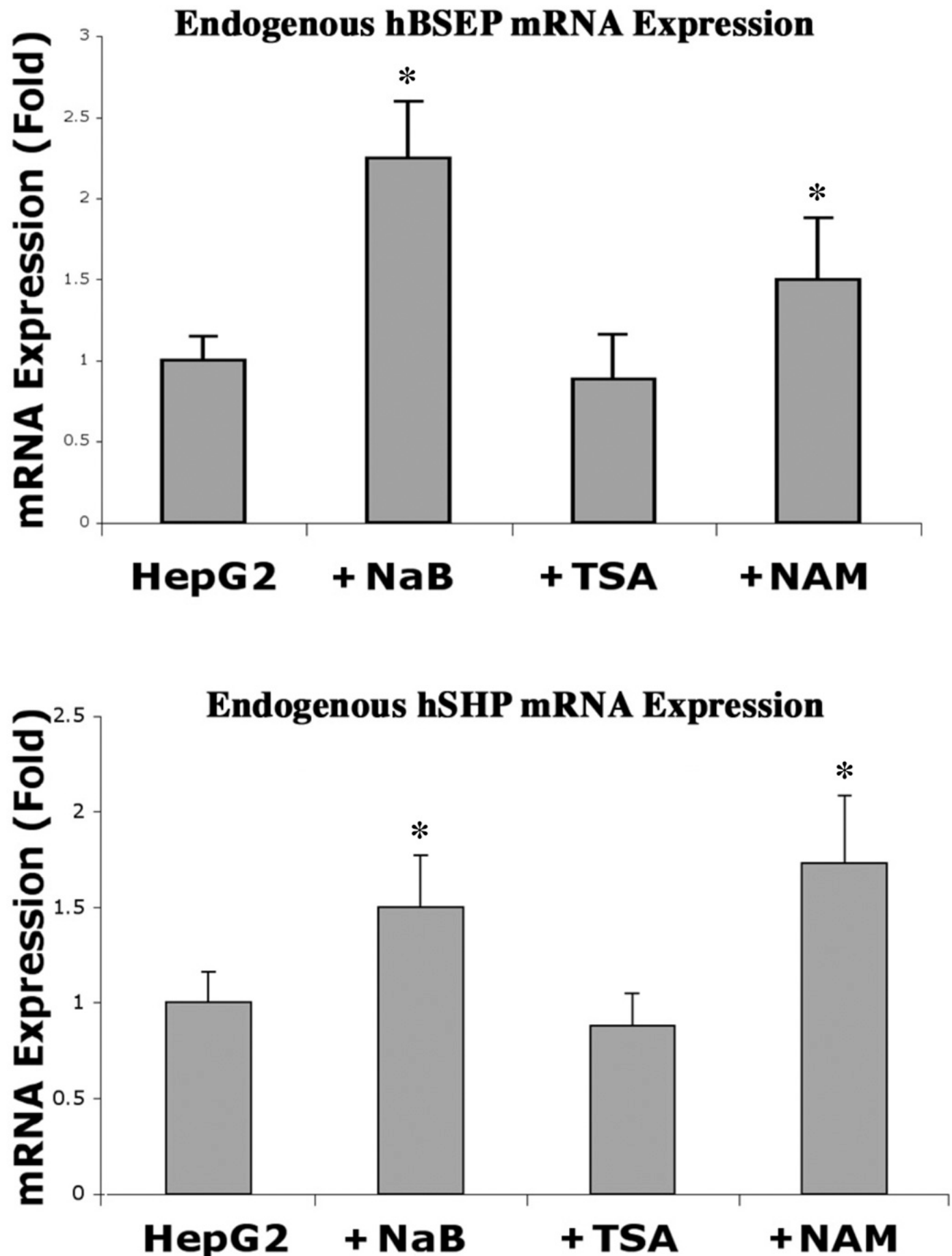


Figure 2

			*122	*157	*206	*210	*213	*237	*275	*339	*460	
Human	1	MGS..GRIKGDE..SITKNAV..CKSKRLRKNV-KQHA..STTKSCR..KILKEEF..FNKKLPS..NDHKFTP...DVQ	472	472	472	472	472	472	472	472	472	472
Monkey	1	MGS..GRIKGDE..SITKNAV..CKSKRLRKNV-KQHA..STTKSCR..KILKEEF..FNKKLPS..NDHKFTP...DVQ	472	472	472	472	472	472	472	472	472	472
Chimpanzee	1	MVM..GRIKGDE..SITKNAV..CKSKRLRKNV-KQHA..STTKSCR..KILKEEF..FNKKLPS..NDHKFTP...DVQ	482	482	482	482	482	482	482	482	482	482
Wolf	1	MGS..GRIKGDE..SITKNAV..CKSKRLRKNV-KQHA..STTKSCR..KILKEEF..FNKKLPA..NDHKFTP...DVQ	476	476	476	476	476	476	476	476	476	476
Rat	1	---..GRIKGDE..SITKNAV..CKSKRLRKNV-KQHA..STTKLCR..KILKEEF..FNKKLPA..NDHKFTP...DVQ	476	476	476	476	476	476	476	476	476	476
Hamster	1	---..GRIKGDE..SITKNAV..CKSKRLRKNV-KQHA..STTKSCR..KILKEEF..FNKKLPA..NDHKFTP...DVQ	469	469	469	469	469	469	469	469	469	469
Mouse	1	---..GRIKGDE..SITKNAV..CKSKRLRKNV-KQHA..STTKFCR..KILKEEF..FNKKLPA..NDHKFTP...DVQ	473	473	473	473	473	473	473	473	473	473
Pig	1	MGS..GRIKGDE..SITKNAV..CKSKRLRKNV-KQHA..STTKSCR..KILKEEF..FNKKLPA..NDHKFTP...DVQ	474	474	474	474	474	474	474	474	474	474
Rabbit	1	MVM..GRIKGDE..SITKNAV..CKSKRLRKNV-KQHA..STTKSCR..KILKEEF..FNKKLPV..NDHKFTP...DVQ	471	471	471	471	471	471	471	471	471	471
Panda	1	MGS..GRIKGDE..SITKNAV..CKSKRLRKNV-KQHA..STTKSCR..KILKEEF..FNKKLPA..NDHKFTP...DVQ	482	482	482	482	482	482	482	482	482	482
Horse	1	MGS..GRIKGDE..SITKNAV..CKSKRLRKNV-KQHA..STTKSCR..KILKEEF..FNKKLPA..NDHKFTP...DVQ	472	472	472	472	472	472	472	472	472	472
Elephant	1	MGS..GRIKGDE..SITKNAV..CKSKRLRKNV-KQHA..STTKSCR..KILKEEF..FNKKLPA..NDHKFTP...DVQ	476	476	476	476	476	476	476	476	476	476

Figure 3

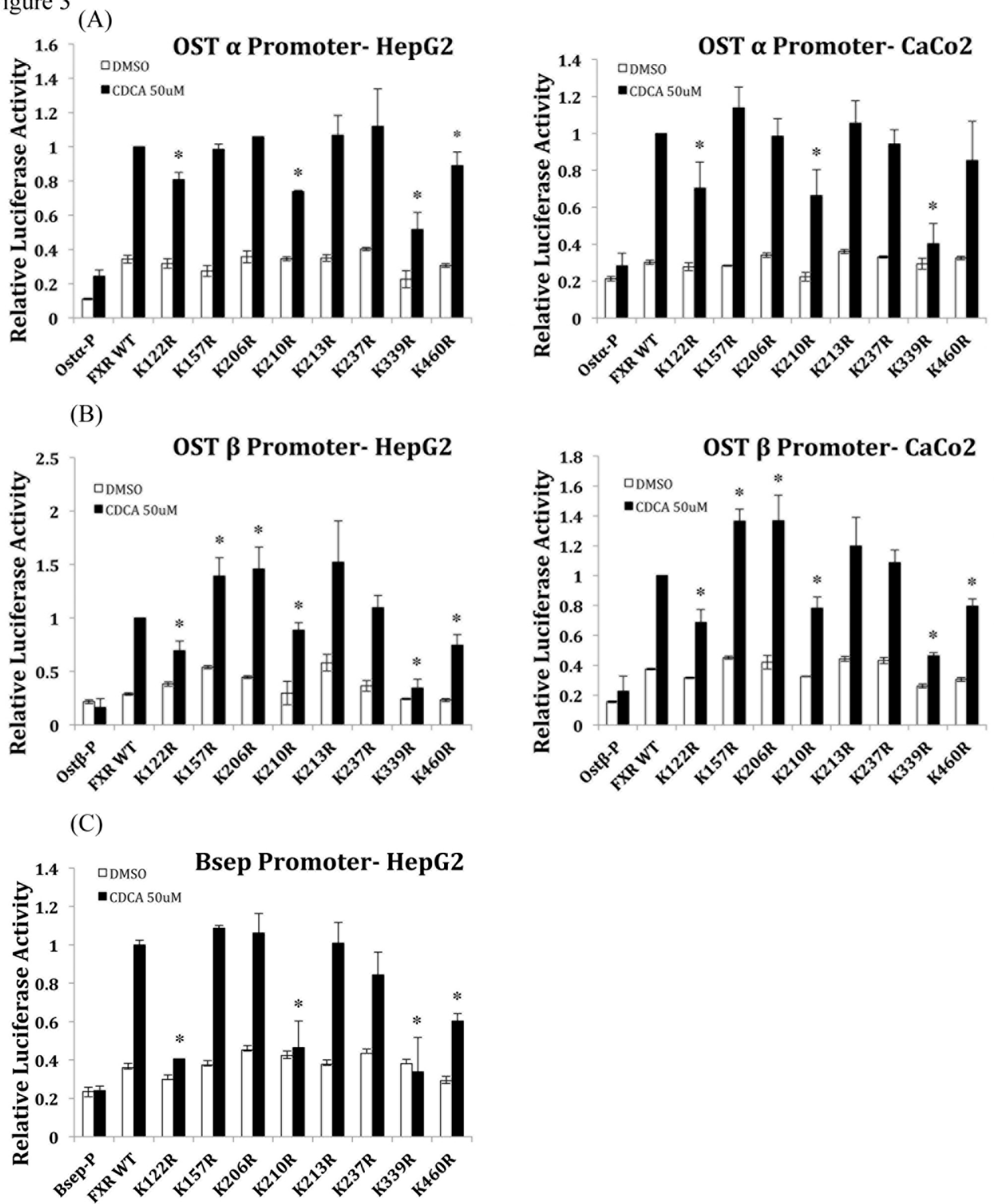


Figure 4

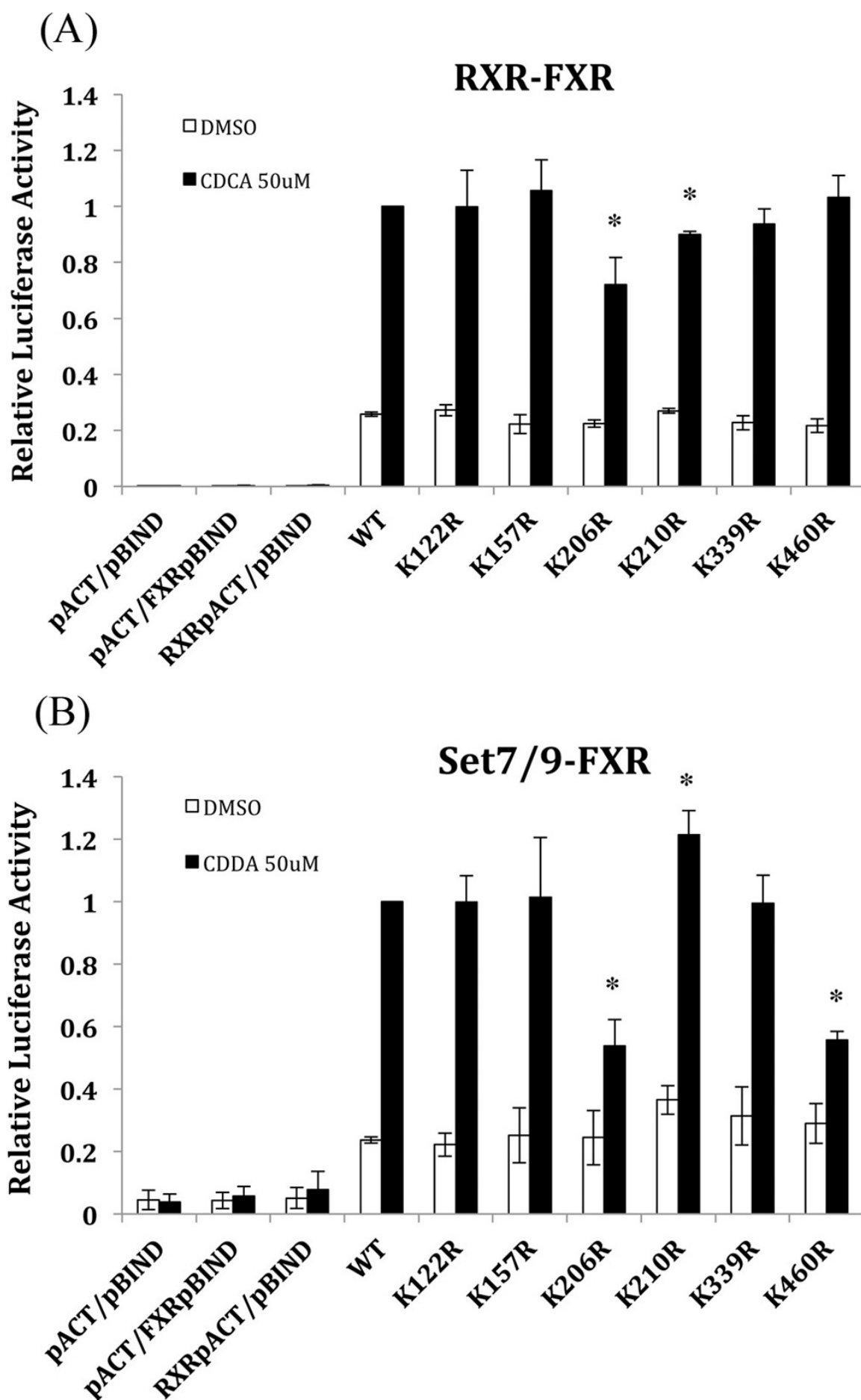


Figure 5

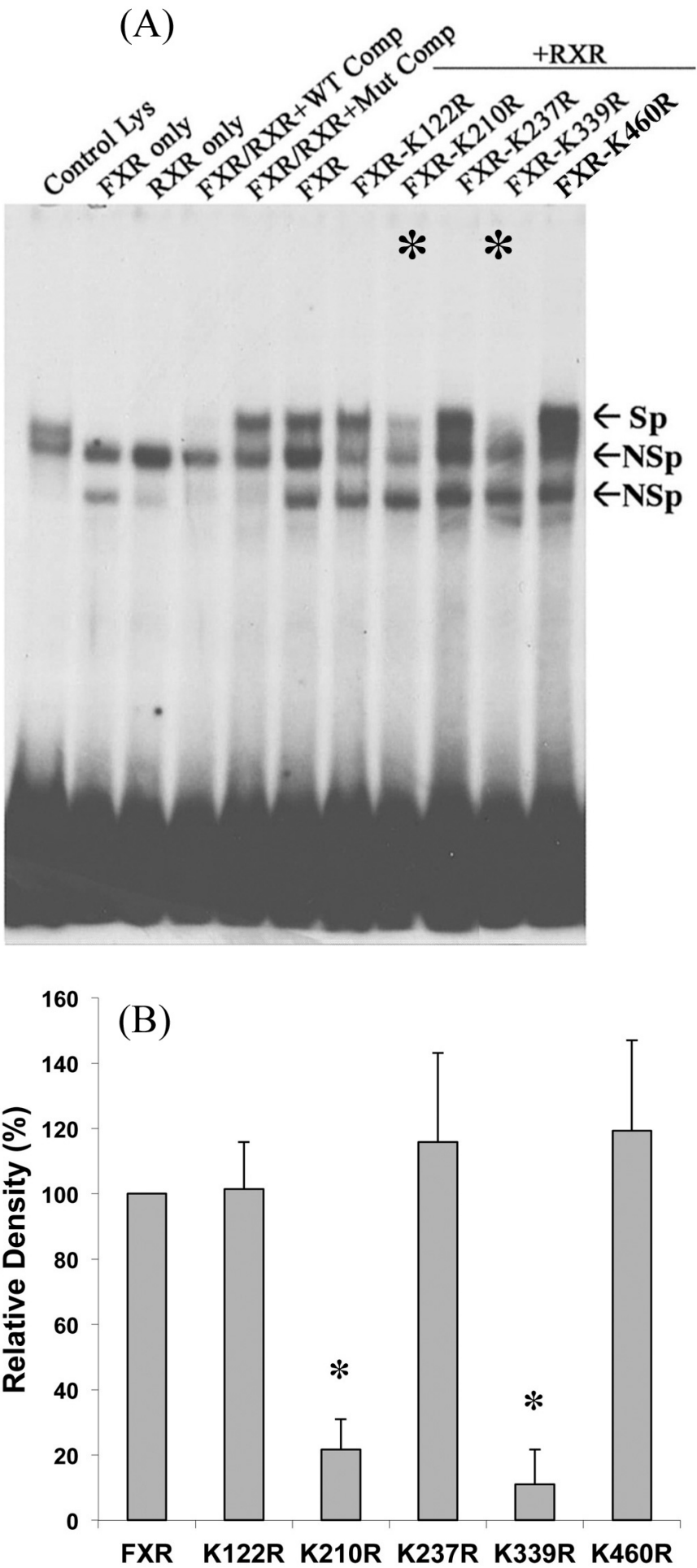


Figure 6

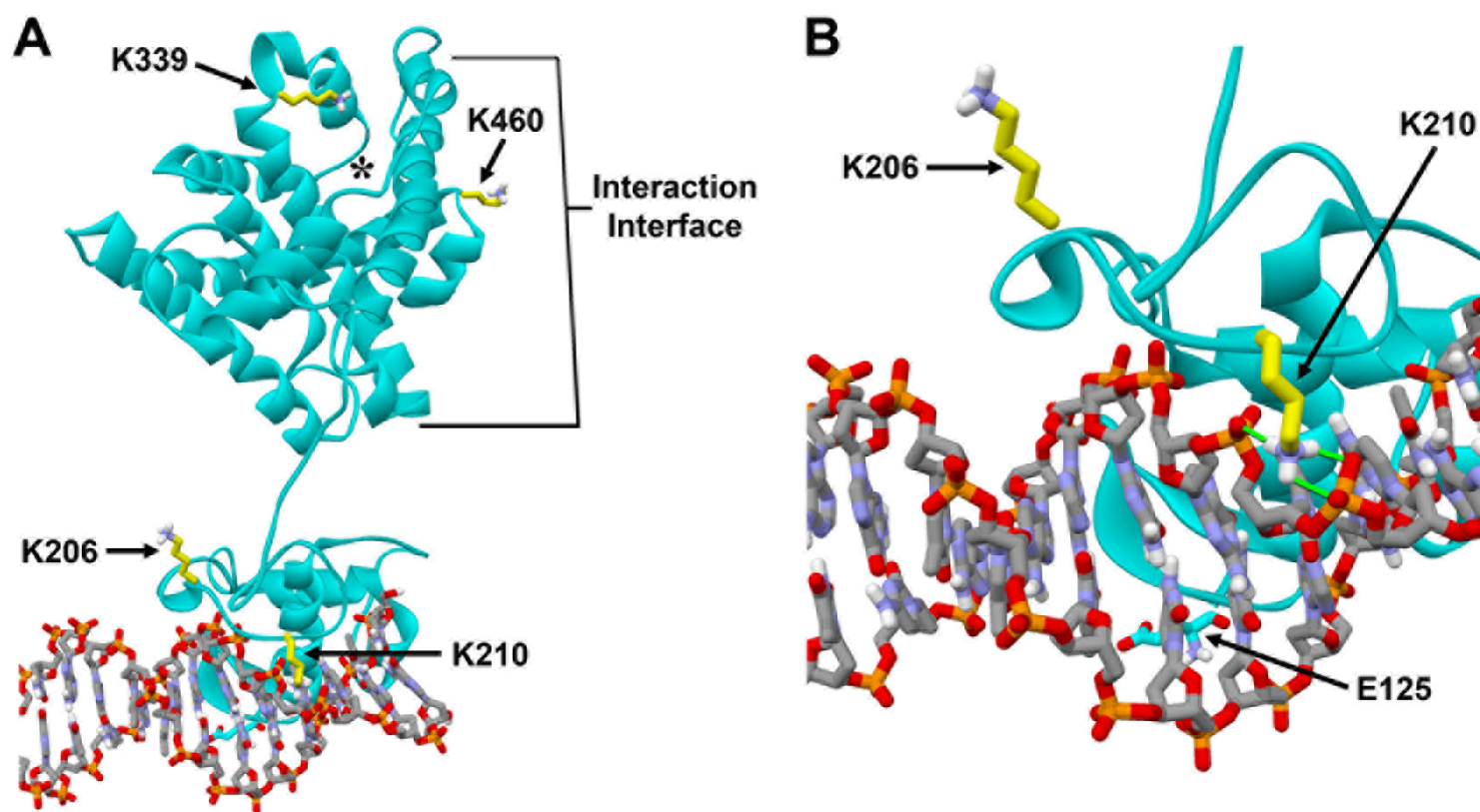


Figure 7

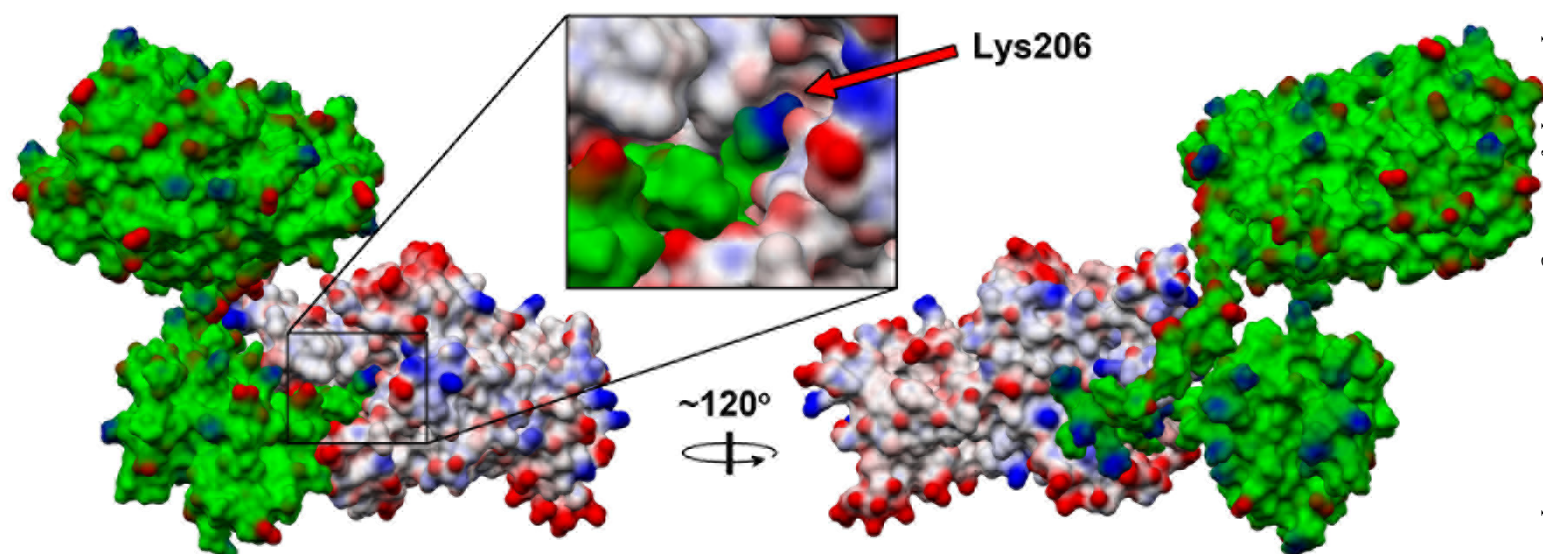


Figure 8

